Anal Bioanal Chem (2014) 406:6903–6916
DOI 10.1007/s00216-014-7895-4

REVIEW

Recent progress in graphene-material-based optical sensors

Xianghua Deng · Hao Tang · Jianhui Jiang

Received: 31 March 2014 / Revised: 7 May 2014 / Accepted: 13 May 2014 / Published online: 1 June 2014

Abstract Graphene material has been widely used for optical sensors owing to its excellent properties, including high-energy transfer efficiency, large surface area, and great biocompatibility. Different analytes such as nucleic acids, proteins, and small molecules can be detected by graphene-material-based optical sensors. This review provides a comprehensive discussion of graphene-material-based optical sensors focusing on detection mechanisms and biosensor designs. Challenges and future perspectives for graphene-material-based optical sensors are also presented.

Keywords Graphene material · Graphene oxide · Optical sensor · Fluorescence resonance energy transfer

Introduction

Graphene is a single-layer sheet structure composed of sp^2-hybridized carbon atoms arranged in a honeycomb lattice [1]. Since it was first isolated via peeling graphite with adhesive in 2004 by Andre Geim and Konstantin Novoselov, who were awarded the Nobel Prize in Physics 2010 for this creative work [2, 3], graphene has emerged as a rising star in materials science owing to its excellent physical and chemical properties. Graphene material has been widely used in the fields of nanoelectronics, catalysis, field-emission displays, composite materials, energy storage, transparent conductors, and biomedicine [4–8]. It has also been proven to be an extraordinary material in chemo/biosensing research, owing to its large surface area, high electron transfer rate, high quenching ability, and excellent biocompatibility. Several critical review articles covering the topic of graphene-material-based sensors are worth reading [9–12]. A graphene-material-based optical sensor is one particular application, and has already achieved great success in recent years. These sensors benefit from the excellent optical properties of graphene material and are generally designed with an energy transfer mechanism. There have been some critical reviews in this area and they provide very useful information for researchers [13–15]. For example, the review by Morales-Narváez and Merkoçi [13] in 2012 discussed different potentially exploitable properties of graphene oxide (GO) structures and presented an overview of the approaches for optical biosensing applications. The review provides valuable information, including a comprehensive summary of the photoluminescence properties and quenching abilities of different GO fabrication processes and structures. In this review, we focus on discussion of the biosensor design principle and detection mechanism, which are mainly based on energy transfer and the interaction of biomolecules with graphene material. We will also discuss graphene-material-based aqueous-phase and solid-phase sensing systems. In addition, the content of graphene–plasmonic hybrid material will be discussed.

Energy transfer of graphene material

Fluorescence resonance energy transfer (FRET) is a nonradiative energy transfer phenomenon which occurs when for two molecules in close proximity there is overlap between the emission spectrum of the donor fluorophore and the absorption spectrum of the acceptor; the effective distance is often in the range of 10 nm or less [16, 17]. FRET has been widely used for biosensing with different materials, such as

Published in the topical collection *Graphene in Analytics* with guest editors Martin Pumera, Ronen Polsky, and Craig Banks.

X. Deng · H. Tang (✉) · J. Jiang (✉)
State Key Laboratory of Chemo/Biosensing and Chemometrics, College of Chemistry and Chemical Engineering, Hunan University, Changsha 410082, Hunan, China
e-mail: haotang@hnu.edu.cn
e-mail: jianhuijiang@hnu.edu.cn

gold nanoparticles (AuNPs), carbon nanotubes, and graphene materials. Compared with other materials, graphene material has many advantages for FRET sensors:

1. The large planar surface structure makes graphene material an excellent energy acceptor with very high quenching efficiency. It has been reported that GO can reach up to 100 % quenching efficiency [18, 19]. Compared with other carbon materials such as graphite, carbon nanotubes, and carbon nanofibers, GO is a better quencher for FRET biosensors [20–22].
2. Benefiting from its structural characteristics, graphene material can quench different excitation wavelengths from different fluorophores. It is a universal quenching material, which broadens its application range. Besides, the large surface area allows adsorption of different fluorescent probes, so it can be applied for multiple probes and multicolor detection.
3. Graphene material can be easily connected to biomolecules by π–π stacking and hydrophobic interactions. Moreover, the graphene derivative GO is a partially oxidized product of graphene which bears a large number of oxygen-containing functional groups, such as hydroxyl, epoxy, and carboxyl groups, located on the edge and surface of the sheet. These functional groups make GO water-soluble and biocompatible as well as the giving it the ability to covalently bond to biomolecules.

Graphene material breaks the FRET distance barrier of donor and accepter molecules. Typically, the efficiency of the FRET process (E) is inversely proportional to the sixth power of the distance between the donor and the acceptor (d): $E=1/[1+(d/d_0)^6]$, where d_0 is the distance at which half of the energy is transferred, and depends on the spectral properties and orientations of the donor and the acceptor [23, 24]. So the effective distance is within 10 nm, and this makes analysis of large proteins difficult. However, graphene with a quenching distance of up to 30 nm has been reported, with an inverse dependence on the fourth power of the distance rather than the sixth power [25–27]. Theoretical calculations suggest the inverse dependence of the energy transfer efficiency on the fourth power of the distance follows a nanometal surface energy transfer mechanism, which is very similar to energy transfer to AuNPs. This type of energy transfer might occur because of the similarity of the graphene structure with the structure of the metal surface. However, most authors tend to refer to the energy transfer process as the well-known FRET process. It might be useful to gain better understanding of the energy transfer mechanisms of graphene material to provide better insight for researchers to design graphene-material-based optical sensors.

Graphene material as a fluorescence acceptor for optical sensors

Energy-transfer-based sensors such as FRET sensors are mainly composed of three parts: donor, acceptor, and bridge group. For graphene quenching sensors, graphene material is used as an energy acceptor, and GO is the most widely used material among of all the graphene materials owing to its advantages of water solubility and bearing functional groups, so this section mainly discusses GO-based quenching sensors. The bridge group can be many kinds of different molecules, including nucleic acids, proteins, and peptides, and the targets can be nucleic acids, proteins, and small molecules. Fluorescence signal transduction is generally induced by a change in the distance between the donor and the acceptor in the presence of target molecules interacting with the bridge group. Since GO has excellent quenching ability for donors with different emission wavelengths, many types of donor materials, such as fluorescent organic dyes, quantum dots (QDs), silver nanoclusters (AgNCs), and upconversion nanoparticles (UCNPs), can be used as a fluorescent label for sensor design. Organic dyes are a simple means to produce a fluorescent label and have been widely used in GO-based FRET assays. Nevertheless, these organic dyes might suffer from photobleaching and photoinstability. As a result, there have been many attempts to use new fluorophores in biosensor areas. Various kinds of nanomaterials have been used to serve as efficient fluorescent labels for GO-based optical sensors, such as AgNCs, QDs, and UCNPs. They have shown advantages as fluorophores over traditional organic dyes owing to their attractive optical and chemical features such as high resistance to photobleaching, stable fluorescence, good biocompatibility, water solubility, and high quantum yield. In this section, we will discuss sensor design methods and applications based on different bridge groups.

DNA as a bridge group

DNA can be adsorbed onto the GO surface via π–π stacking interaction between nucleobases of the DNA and the sp^2-hydridized atoms of the GO nanosheet or through covalent bonding. When the fluorescently labeled DNA probe and GO are brought close to one another, the fluorescence from the fluorophore can be quenched by GO. The fluorescence can be restored after the target DNA interacts with the DNA probe to take the fluorophore away from the GO surface. The sensing strategy follows this basic principle by using DNA as probe to develop GO-based FRET optical sensors.

Sensors based on DNA hybridization

GO has different affinities toward single-stranded DNA (ssDNA) and double-stranded DNA (dsDNA). Single-

stranded DNA (ssDNA) can easily adsorb GO via π–π stacking interaction between nucleobases of the DNA and the sp^2-hybridized atoms of the GO nanosheet. On the other hand, GO binds more weakly with dsDNA because the negatively charged phosphate can efficiently shield nucleobases from GO and weaken the π–π stacking interaction. Lu et al. [28] have reported a GO-based FRET sensor utilizing this mechanism. The fluorescence of fluorescein amidite (FAM)-labeled ssDNA which was designed as a complementary sequence with target DNA was quenched efficiently owing to the high quenching efficiency when it was adsorbed onto the GO surface. In the presence of target DNA, the dsDNA formed left the surface of GO, and fluorescence recovery was observed (Fig. 1a). This simple approach resulted in good sensitivity for DNA detection owing to the high quenching efficiency of GO.

Because organic dyes might suffer from photobleaching and photoinstability, different labeling approaches have been developed. AgNCs have advantages such as high luminescence quantum yields, tunable emissions controlled by their size, good photostability, water solubility, biocompatibility, and low toxicity. A GO-based biosensor using a DNA-templated AgNC probe has been developed. The AgNCs were synthesized in solution using ssDNA as a template, and the fluorescence of AgNCs was quenched by GO when the ssDNA probe was adsorbed onto the surface. Fluorescence was recovered when the target DNA hybridized with the probe [31]. Furthermore, QDs are excellent fluorescent labels for a GO-based sensor owing to their broad absorption and narrow emission spectra [32]. Since the large surface area of GO allows adsorption of many probe molecules, rapid, sensitive, and multicolor fluorescent DNA analysis can be realized [33–37]. The approaches using noncovalent π–π stacking interaction to adsorb DNA probes onto GO surfaces have many advantages, such as high sensitivity and a simple adsorption process. However, this approach might suffer from weak selectivity, and this might limit its application for complicated biological samples because extensive ssDNA probe loading onto GO might cause nonspecific strand displacement by nonspecific ssDNA. In this case, a false signal will be induced by nontarget DNA molecules. On the other hand, low loading of the ssDNA probe onto GO might cause target DNA to adsorb on unoccupied sites on the GO surface, and the sensitivity would be impaired to some extent.

The nonspecific ssDNA displacement effect can be improved using a DNA probe with a sticky end structure. The sticky end is typically a dangling sequence several nucleotides in length and is usually used as a toehold which can regulate well DNA strand displacement. Recently, Miyahata et al. [29] developed a senor based on toehold-mediated fluorescent DNA strand exchange on GO. The fluorescent dye moiety of the probe DNA was placed near GO through a capture DNA. When targets were added, the probes were released from the GO through toehold-mediated strand exchange to recover fluorescence (Fig. 1b). This approach had improved selectivity compared with direct adsorption–desorption of the fluorescent ssDNA probe since the nonspecific strand displacement effect could be eliminated. Similarly, Huang et al. [38] have reported GO-quenched dye-labeled DNA hairpin probes designed by using the sticky end structure for hybridization chain reaction. This design could help eliminate nonspecific strand displacement and could also be combined with a signal amplification strategy to improve sensitivity.

Another approach is to covalently immobilize an ssDNA probe on GO [30, 39, 40]. This strategy can eliminate nonspecific probe displacement and is more suitable when dealing with complicated biological samples (Fig. 1c). Besides, it can be used to monitor continuous processes, which would be very difficult to realize by noncovalent π–π stacking interaction adsorption since after hybridization with the target, the dsDNA will leave the surface of GO. Owing to the functional groups on the surface of GO such as –OH and –COOH, covalent bonding can be easily realized. Huang and Liu [30] covalently attached a molecular beacon onto the GO surface using *N*-ethyl-*N*′-[3-(dimethylamino)propyl]carbodiimide hydrochloride as a coupling agent. The covalent probe has the advantage of allowing detection in a complex biological sample matrix because the strong covalent bonding can minimize nonspecific probe displacement.

Sensors based on aptamer recognition

Aptamers are selected short single-stranded oligonucleotides which have highly specific affinity for proteins, small molecules, or ions. An aptamer-based GO sensor can be used to detect many different analytes owing to the recognition ability of the aptamer. A general design principle is to use a fluorescently labeled aptamer. The fluorescence is quenched by GO since it has strong affinity for ssDNA, and after recognition of the target, the conformational change of the aptamer can cause the fluorophore to move away from the GO surface, resulting in recovery of fluorescence. Chang et al. [41] demonstrated this mechanism with thrombin detection. A FAM-labeled thrombin aptamer was first adsorbed onto the GO surface, and so the fluorescence was quenched. Thrombin combined with the aptamer to induce a G-quadruplex complex to allow FAM to move away from GO since GO has strong affinity for ssDNA but less affinity when the nucleobases are shielded in dsDNA or a complicated DNA structure (Fig. 2a).

UCNPs have the ability to fluorescence strongly in the visible region under excitation by near-IR (NIR) light, which would not be absorbed by biological samples, and the autofluorescence background can be minimized. Detection of different analytes has been realized by a GO–aptamer

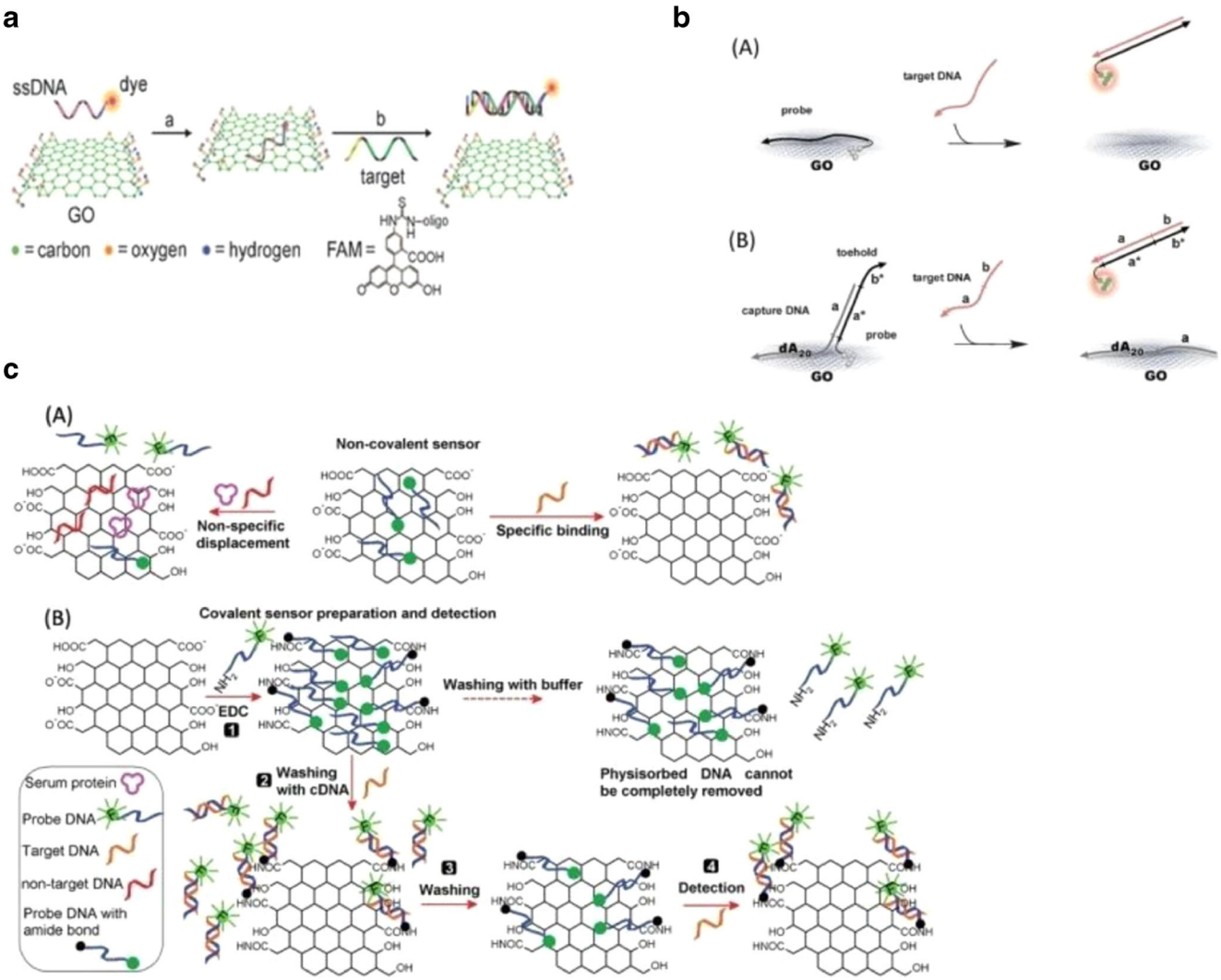

Fig. 1 Sensor based on DNA hybridization. **a** The fluorescence of a fluorescein amidite (*FAM*)-labeled single-stranded DNA (*ssDNA*) probe was nearly completely quenched when it was adsorbed onto the graphene oxide (*GO*) surface via π–π stacking interaction. In the presence of target ssDNA, the interaction between GO and the dsDNA is weaker, so the dsDNA was desorbed and the FAM emission was restored. **b** GO-based DNA sensing systems using direct adsorption–desorption of the fluorescent DNA probe (*A*) and the indirect toehold-mediated strand displacement approach (*B*). **c** A noncovalent sensor which might generate a false signal by probe displacement or a true signal by forming dsDNA (*A*). Covalently linking amino-modified DNA to GO can be achieved by *N*-ethyl-*N*′-[3-(dimethylamino)propyl]carbodiimide hydrochloride (*EDC*) coupling (step *1*), but only a fraction of the DNA is covalently attached, and the remaining DNA is physisorbed (*B*). Washing in buffer cannot completely remove physisorbed DNA, and complete desorption requires washing with complementary DNA (*cDNA*; step *2*). The cDNA needs to be washed away (step *3*). The covalent sensor can be used for detection (step *4*). It is likely that some of the cDNA also remains on the GO surface after washing without interfering with the detection. (**a** From [28], copyright 2009 Wiley-VCH Verlag GmbH & Co. KGaA; **b** adapted from [29] with permission, copyright 2013 Royal Society of Chemistry; **c** from [30], copyright 2012 American Chemical Society)

platform using different labels such as UPNCs, AgNCs, and QDs [42–45]. Besides, a two-photon fluorescent dye has been reported for a GO–aptamer-based FRET optical sensor in vitro and in vivo assay which can effectively reduce the self-absorption, autofluorescence, and photodamage [46]. The GO–aptamer approach has the advantages of high sensitivity and selectivity owing to the high efficiency of GO and the high affinity of aptamers [47–51]. In addition, different fluorophore-labeled aptamers could be adsorbed onto GO surfaces to achieve multiplexed analysis [42, 52–54]. Liu et al. [42] have developed an AgNC and GO system for the multiplexed analysis of genes, including the hepatitis B virus gene, the human immunodeficiency virus gene, and the syphilis (*Treponema pallidum*) gene, based on DNA hybridization, and of ATP or thrombin based on aptamer recognition. Owing to their size-controlled fluorescent property, red-emitting AgNCs (616 nm) and NIR-emitting AgNCs (775 nm) could be used (Fig. 2b). It is envisioned that, owing to the development of the systematic evolution of ligands by exponential enrichment (SELEX) method, more aptamers for more biomolecules will be selected and the application of GO–aptamer sensors will be broadened.

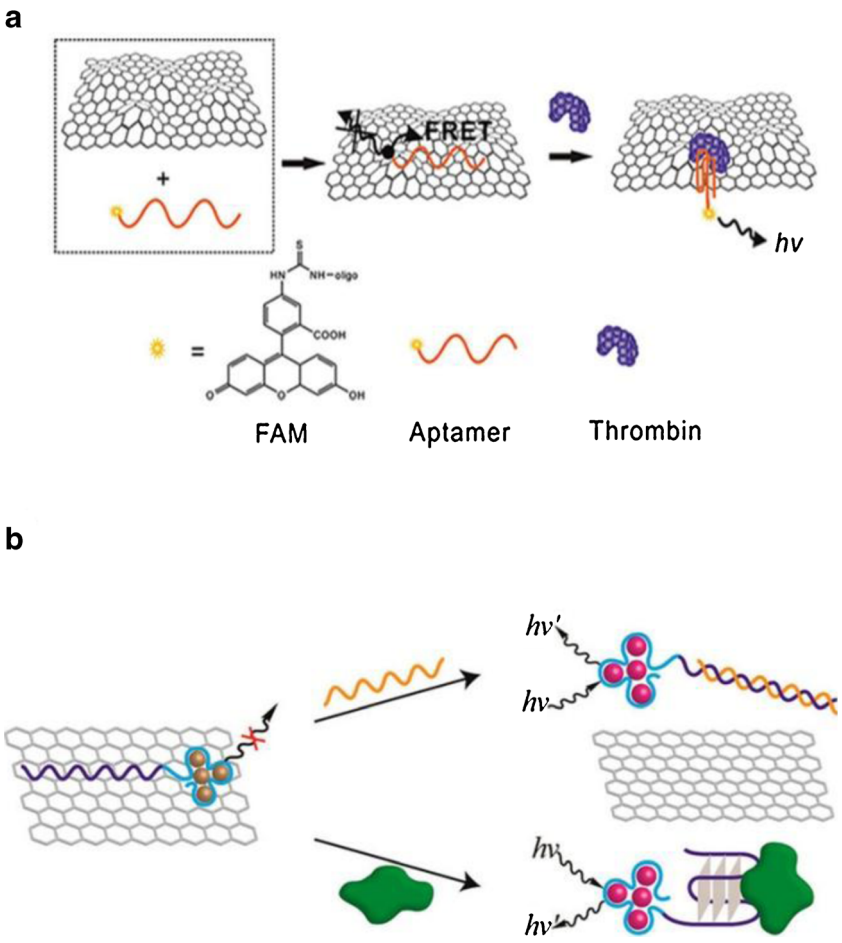

Fig. 2 **a** A graphene fluorescence resonance energy transfer (*FRET*) aptasensor and the detection mechanism for thrombin. Fluorescence of the dye-labeled aptamer is quenched when the aptamer binds to graphene owing to FRET between the dye and graphene. The fluorescence recovers when thrombin combines with aptamers to form a G-quadruplex complex, which has much less affinity for graphene, causing FAM to move far away from the graphene surface. **b** Assay of the target DNAs using DNA-templated silver nanocluster (AgNC)–GO hybrids and proteins using an aptamer-elongated DNA–AgNC–GO hybrid system as sensing matrices. (**a** From [41], copyright 2010 American Chemical Society; **b** from [42], copyright 2013 American Chemical Society)

Sensors based on metal ion and mismatched DNA recognition

Besides the previously discussed conformational change induced by DNA hybridization and aptamer–target recognition, a metal ion is another way to introduce a change in the conformation of DNA. It has been demonstrated that some mismatched DNA base pairs can selectively form a complex with certain metal ions owing to their strong affinity. Many GO-based quenching sensors have been developed for metal ions and targets. This type of sensor is generally based on interaction between mismatched DNA and analytes, which are metal ions in most situations. The metal–DNA complex can induce the conformational change of the DNA probe and cause the fluorophore to move away from the GO surface, so the fluorescence signal would change in the presence of metal ions. For example, thymine has been reported as a specific ligand for Hg^{2+} to form thymine–Hg^{2+}–thymine base pairs [55, 56] owing to the strong interaction. Similarly, Ag^{+} and cytosine can form a cytosine–Ag^{+}–cytosine duplex [57, 58]. Several biosensors have been developed using this design; the analytes include Hg^{2+}, Ag^{+}, and biothiols [59–62].

Wen et al. [59] reported a FRET sensor based on a cytosine-rich DNA probe and GO. In the presence of Ag^{+}, a DNA–Ag^{+} complex was formed, and the conformation of the probe changed to straight stiff dsDNA, resulting in desorption of DNA from the surface of GO and fluorescence recovery (Fig. 3a). Gao et al. [60] developed a GO-based fluorescent probe to quantitatively analyze biothiols. They used fluorescein isothiocyanate labeled ssDNA rich in thymine bases. The addition of Hg^{2+} resulted in the formation of thymine–Hg^{2+}–thymine and a self-hybridized duplex structure in dsDNA to keep FAM away from the surface of GO; thus, Hg^{2+} led to a large amount of fluorescence recovery. Since biothiols have high affinity for heavy metal ions, especially Hg^{2+}, the selectively competitive binding of Hg^{2+} between thiols can cause the duplex DNA structure to revert to ssDNA, resulting in fluorescence quenching (Fig. 3b).

These approaches provided a homogeneous assay for convenient, rapid, robust, and sensitive detection of metal ions such as Hg^{2+} and Ag^{+}. Also, small molecules such as biothiols and cysteine which can interact with these metal ions can be detected. These sensors have a wide linear range, and the detection limits for metal ions can reach down to the nanomolar to subnanomolar range, which is suitable for analysis of environmental and biological samples.

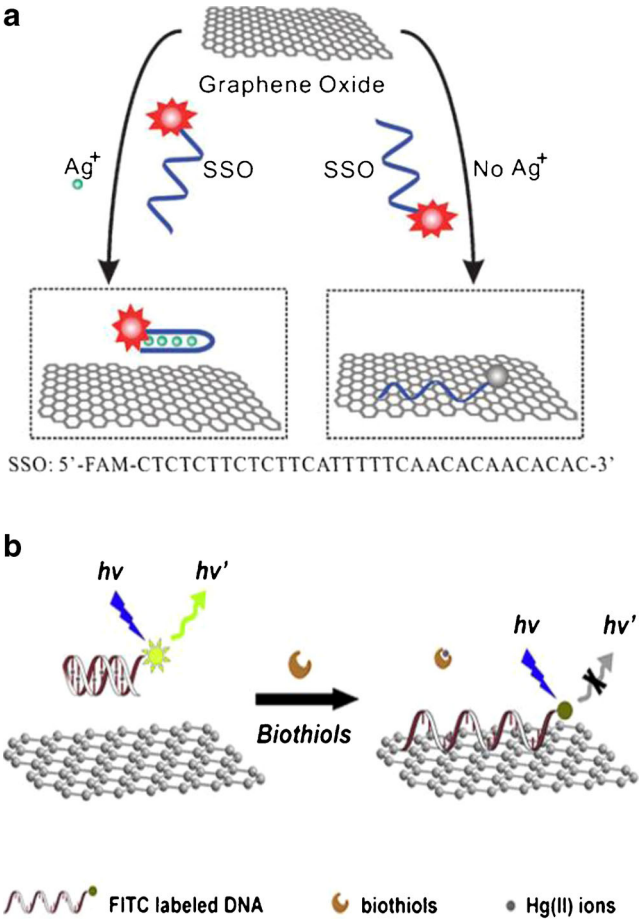

Fig. 3 **a** A FRET sensor for Ag(I) ions based on the target-induced conformational change of a FAM-labeled silver-specific cytosine-rich oligonucleotide (*SSO*) and interaction between the fluorogenic SSO probe and GO. **b** A GO-based molecular-beacon-like probe for biothiol analysis. (**a** From [59], copyright 2010 Royal Society of Chemistry; **b** from [60], copyright 2012 Elsevier)

Sensors based on DNAzymes

Since 1990, some DNA molecules referred to as DNAzymes, catalytic DNAs, or deoxyribozymes have been reported to possess a unique catalytic activity toward specific substrates when combined with metal ions [63, 64]. Several types of metal ion sensors have been developed based on FRET, including Cu^{2+}, Pb^{2+}, and Hg^{2+} sensors [65–67]. These types of sensors often used a DNA probe labeled with both a fluorophore and a quenching group as a substrate of DNAzymes, so first the fluorescence is quenched. DNAzymes selectively combine with a metal ion to catalyze cleavage of the DNA probe, so free fluorophores are released, leading to fluorescence recovery. Along with the development of graphene material, GO combined with a DNAzyme platform has been developed for detection of different metal ions [68–70].

Compared with methods using both fluorophore and quenching group labels, GO-based sensors have the advantages of higher quenching efficiency and a simpler labeling process, and some label-free approaches can also be achieved. For example, Liu et al. [68] have developed a "turn -on" sensor for Cu^{2+} based on the change in the conformation of GO–DNAzyme in the presence of Cu^{2+} (Fig. 4a). Benefiting from the high quenching efficiency of GO, the limit of detection based on this method was 0.4 nM, which was better than that of the previous Cu^{2+}-dependent DNAzyme sensors [71, 72]. Label-free GO–DNAzyme-based fluorescent biosensors have been developed for detection of Cu^{2+} by Liu et al. [70]. They extrinsically intercalated the fluorophore into the DNAzymes, which contain duplex and triplex regions. Then, the fluorescence of the self-assembled GO–DNAzyme complex was quenched. When the target Cu^{2+} was subjected to the sensing system, the fluorescence signal was recovered (Fig. 4b). Since numerous types of DNAzymes have been selected to bind a wide range of metal ions, the GO–DNAzyme system provides a new general homogeneous optical platform for sensitive (nanomolar to subnanomolar detection limit) and selective detection of various metal ions.

Sensors based on DNA signal amplification

Although GO has great quenching ability, the sensitivity for DNA detection is normally limited to the nanomolar range when a signal amplification approach is not used [13]. This sensitivity is suitable for many applications, but for some applications, such as clinical diagnosis, gene therapy, and mutation analysis, ultrasensitive detection of DNA is important.

One approach is to load a large amount of fluorescent labels, but this would increase the cost of the labeling process and the time required. Another way is based on target cycling to amplify the signal. In recent years, several GO-based FRET sensors based on DNA signal amplification approaches have been developed, including exonuclease-mediated amplification [73–76], endonuclease-mediated amplification [77–80], isothermal circular strand displacement amplification [81–84], and hybridization chain reaction [38, 85–87]. Although these methods improved the detection limit to the picomolar level, they often required very careful control and optimization of the enzyme and different DNA probe concentrations. Moreover, these approaches were time-consuming and encountered the problems of complicated procedures, high cost, and false-positive signals. There are still some challenges to be overcome in order to achieve practical applications.

Protein as a bridge group

Immunoassay using antigen–antibody recognition is a well-developed platform for protein detection. The antigen–antibody recognition makes possible highly selective analysis of proteins. Many detection methods have been widely adopted for immunoassay, such as colorimetry, fluorescence labeling, electrochemistry, chemiluminescence, and surface-enhanced

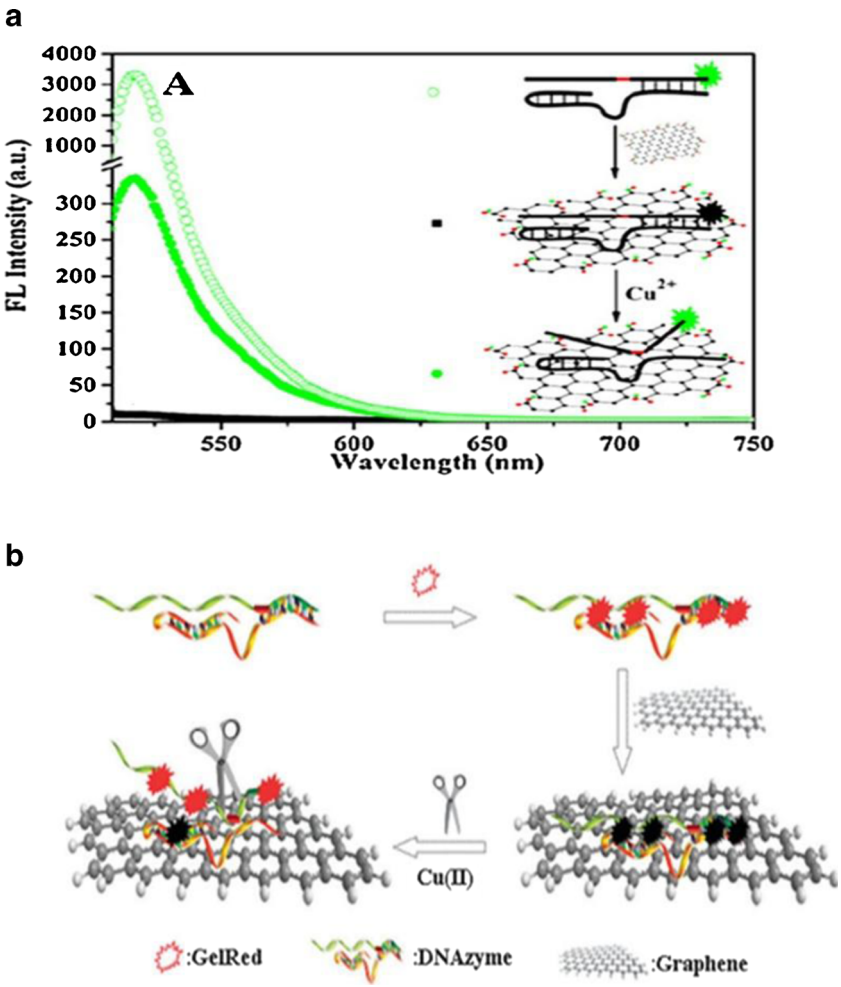

Fig. 4 **a** A "turn-on" fluorescent Cu^{2+} sensor based on a GO–DNAzyme system and steady-state fluorescence spectra of DNAzyme under different conditions. **b** Label-free fluorescent detection of Cu^{2+} based on GO-quenched DNAzyme. *FL* fluorescence. (**a** From [68], copyright 2011 Elsevier; **b** from [70], copyright 2011 Royal Society of Chemistry)

Raman spectroscopy [88–91]. Owing to the extraordinary quenching ability of GO, which can reach a distance up to 30 nm for effective quenching, an antibody or antigen can be used as a bridge group to specifically recognize protein targets [92–94]. The large amounts of carboxyl, hydroxyl, and epoxy groups on the surface of GO sheets allow convenient covalent conjugation with other molecules. For example, Liu et al. [92] developed an ultrasensitive fluorescence immunoassay to detect α-fetoprotein (AFP) based on FRET between CdTe QDs (donor) and GO (acceptor), which broke the distance limit (10 nm) of traditional fluorescent biosensors. The capture antibody (Ab1) was connected to GO sheets via covalent bonding. In the presence of target AFP, because of the self-assembled immunocomplexes (Ab5/AFP/Ab1), the bridge AFP would give rise to several effective orientations or localizations of the immunocomplexes, resulting in the quenching of the emission of the QDs (Fig. 5a).

In addition to antibody–antigen recognition, the reaction between saccharide and protein can be used to build a bridge connection for sensors. Several GO quenching biosensors based on a saccharide and protein bridge have been developed [95, 97, 98]. For example, Zhang et al. [95] developed a novel FRET biosensor platform to detect glucose through specific molecular recognition. In their work, GO covalently attached to chitosan was used as a powerful fluorescence acceptor. UNCPs with covalent attachment of concanavalin A (ConA) were used as an effective fluorescence donor. They were brought close to chitosan by specific molecular recognition interaction between ConA and chitosan, and the fluorescence of UCNPs was quenched by GO. Owing to the competition between glucose and chitosan for ConA, in the presence of glucose, the UCNPs would leave surface of GO and this resulted in recovery of fluorescence (Fig. 5b). UCNPs have the ability to fluorescence strongly in the visible region under excitation by NIR light, which can eliminate the autofluorescence background of biological samples.

For these types of sensors, the unique interactions between protein and graphene material might have a negative effect on the sensor performance because it might cause the protein to lose function and thus be unable to recognize targets. Experiments [99, 100] and simulations [101] have shown that the conformational change and loss of function of the biomolecules would occur while they are covalently or noncovalently connected to the nanomaterial surface because the activity and

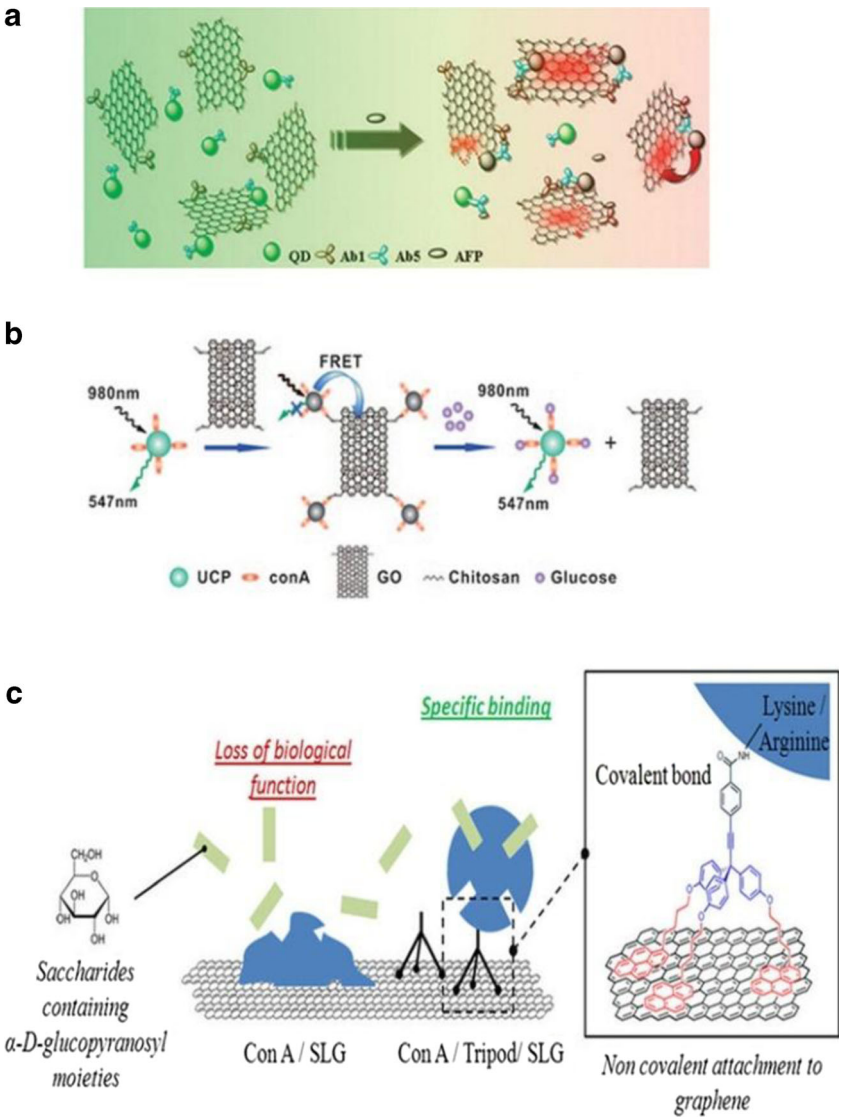

Fig. 5 **a** FRET immunoassay based on self-assembled quantum dots (*QD*) and nanoscale graphene. **b** The GO–upconversion nanoparticle (*UCP*) biosensing platform and the mechanism of glucose determination. **c** Interfacing concanavalin A (*ConA*) with single-layer graphene (*SLG*) and evaluating its biological function. *Ab* antibody, *AFP* α-fetoprotein. (**a** From [92], Copyright 2010 Royal Society of Chemistry; **b** from [95], copyright 2011 Wiley-VCH Verlag GmbH & Co. KGaA; **c** from [96], copyright 2013 American Chemical Society)

selectivity rely on specific tertiary or quaternary structure of biomolecules. Recent work has demonstrated protein function can be effectively preserved by adding a self-assembled monolayer (SAM) between graphene material and protein [96, 102, 103]. The SAM can be large molecules or polymers adsorbed onto the surface of graphene material via π–π stacking or hydrophobic interactions, and they can covalently link to the protein molecule. For example, the function of the protein ConA was preserved by covalently immobilizing ConA onto a SAM of multivalent tripodal molecules which adsorbed on single-layer graphene (Fig. 5c).

Peptide as a bridge group

A peptide is another important bridge group for GO quenching sensors mainly focused on protein or peptidase analysis. For protein detection, peptide–protein interaction is a general design [104–106]. For example, Wang et al. [104] used pyrene-labeled RGD as probe for integrin $\alpha_v\beta_3$ detection. The fluorescence of pyrene was quenched because the probe could adsorb to the GO surface via π–π stacking interaction. After addition of the target, the quenched fluorescence was significantly enhanced by virtue of the competitive binding of the peptide and protein (Fig. 6a). This work used RGD to target cancer cells for intercellular analysis since integrin $\alpha_v\beta_3$ is a general biomarker expressed by cancer cells.

For noncovalent bonding, the interactions are from π–π stacking and the hydrophobic effect. When designing appropriate peptide sequence so the peptide can strongly adsorb on GO, one needs to consider amino acids bearing aromatic rings, such as phenylalanine, histidine, tyrosine, and tryptophan [108]. For analysis of different peptidases, GO–peptide-based biosensors can be constructed by designing different peptide sequences. In this type of sensor there is usually a peptidase cleavage site for peptidase to cleave the fluorophore-labeled peptide to recover the fluorescence

quenched by GO, and both in vitro and intracellular analysis can be achieved [107, 109–111]. For instance, Wang et al. [107] adopted a GO–peptide-based sensor for intracellular caspase-3 activation imaging in living cells. The intracellular protease sensor for high-contrast imaging of apoptotic signaling in living cells was based on intracellular delivery of a GO–peptide conjugate and caspase-3-mediated cleavage of the substrate peptide. First, the fluorescence of the FAM-labeled peptide was quenched, and after the cleavage of the peptide mediated by caspase-3 in the living cell, the FAM label left the GO surface, and so the fluorescence image of the cell could be obtained. Covalent bonding of the peptide and GO was stable in a high-concentration protein medium. According to their results, the noncovalent GO–peptide complex might not serve as an efficient carrier to deliver peptides into cells owing to the desorption of peptides from the GO surface induced by large amounts of protein in the cell culture medium (Fig. 6b).

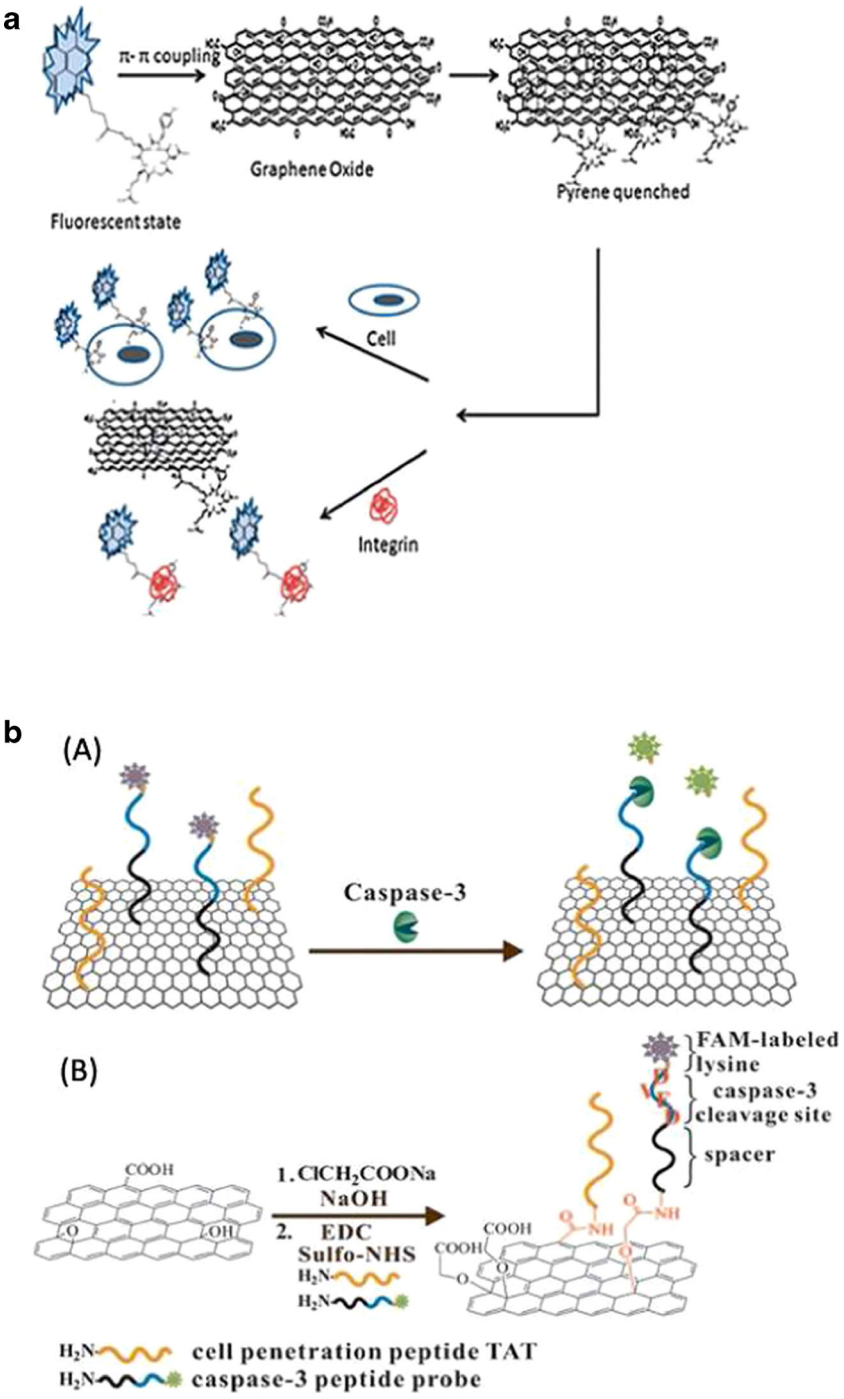

Fig. 6 **a** RGD–pyrene interaction with GO to quench the fluorescence of pyrene, and the recovery of fluorescence by introducing either integrin $\alpha_v\beta_3$ protein or integrin-overexpressing cancer cells. **b** Caspase-3 detection using a GO–peptide conjugate (*A*) and construction of the GO–peptide conjugate (*B*). *Sulfo-NHS N*-hydroxysulfosuccinimide. (**a** From [104], copyright 2012 Royal Society of Chemistry; **b** from [107], copyright 2011 Wiley-VCH Verlag GmbH & Co. KGaA)

Graphene material as a fluorescence donor for optical sensors

Photoluminescence can be induced in graphene material when the size, structure, and surface property are controlled properly [112] as for traditional semiconductor-based QDs. Fluorescent graphene material has great potential for application in bioimaging and drug delivery and can be used for a FRET optical sensor as a donor.

AuNPs can act as effective quenching material for GO, and some biosensors have been developed using this strategy [113–119]. Jung et al. [113] synthesized a fluorescent GO array and covalently connected the array to an antibody, a secondary antibody was labeled with AuNPs, in the presence of the target pathogen, and AuNPs were brought close to the GO array to quench the fluorescence via immunorecognition (Fig. 7). This work illustrates the great potential of GO to be applied for biosensors as a novel fluorescent tag.

Currently, most of the reported fluorescent colors of graphene material are in the visible range [120–122], but if the fluorescence spectra were extended to the NIR and even IR regions, the application area could be expanded greatly. The current challenge is obtaining narrow graphene material with a uniform structure and surface property to control fluorescence. Graphene QDs (GQDs) have attracted great attention in recent years as fluorescent graphene material. GQDs are a zero-dimensional nanomaterial with a size of less than 100 nm [123]. Therefore, GQDs have some unique characteristics associated with graphene and carbon dots such as low cytotoxicity, large surface area, good water solubility, high stability, and high biocompatibility [124–128]. In addition, owing to quantum confinement and edge effects, GQDs are highly luminescent and have lots of different emission wavelengths. Fluorescent GODs have been synthesized. GQDs have been widely used to sense different analytes as an energy donor recently; more information can be found in a review article focusing on GQD-based sensors [129].

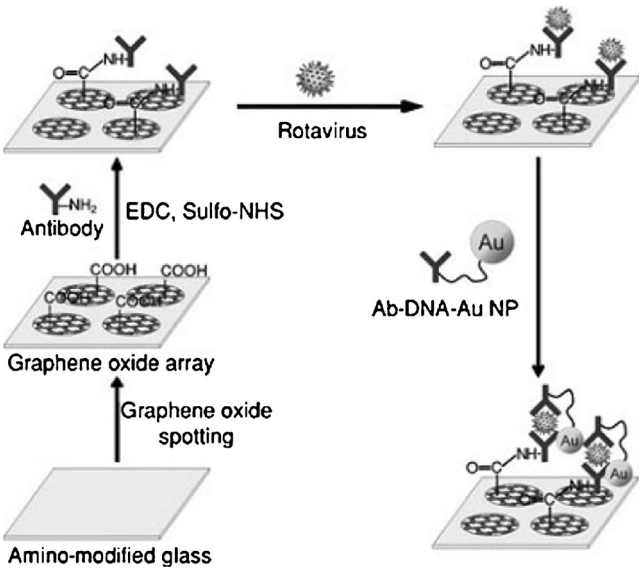

Fig. 7 Analytical principle of the GO-based immunobiosensor. *Ab* antibody, *NP* nanoparticle. (From [113], copyright 2010 Wiley-VCH Verlag GmbH& Co. KGaA)

Graphene material in the solid phase for optical sensors

Most of the previously discussed optical sensors are based on aqueous solution systems because these are simple, convenient, and robust. However, the solution approach is not quite suitable for high-throughput and multiplexed analysis. Microarray technology has become a useful analytical tool for biochemical analysis because of its intrinsic advantages of high-throughput monitoring, small reaction volumes, and multiplex and parallel analysis of many samples in a single chip. For these types of sensors, graphene material or a probe can be fabricated on a solid support to form a microarray type of sensor [130–132]. Morales-Narváez et al. [131] reported a pathogen-detection system using antibody–QD microarrays for pathogen attachment. The free antibody–QD probes extensively interacted with GO through π–π stacking, so when GO was added, the fluorescence of the QDs was quenched. In the presence of the pathogen, the pathogen was selectively captured by the antibody–QD probes; consequently, the bound antibody–QD probes barely interacted with GO, so fluorescence was recovered (Fig. 8a). This pathogen-detection system is highly sensitive for *Escherichia coli* in phosphate-buffered saline and in tap water and might be extended to detect other types of analytes (e.g., cancer cells) [131].

Another approach is to print GO layers onto a given substrate. Because micrometer-sized GO is too large and has a planar structure, the spotting method using a microarray spotter is challenging. Layer-by-layer assembly has been adopted for the immobilization of GO on a solid glass substrate because this method is versatile and highly tunable to form thin films via alternating adsorption of positively and negatively charged species on the substrate [133–136]. Jung et al. [133] fabricated multilayer GO on an amine glass substrate using electrostatic interaction; the number of layers was tunable (Fig. 8b). The limit of detection for human thrombin with a ten-bilayer GO array is estimated to be 0.001 nM, which is 30-fold more sensitive than a solution-based graphene FRET aptasensor [41]. A solid-phase microarray of graphene material optical sensors has the advantages of low sample consumption and high-throughput analysis ability; however, this approach requires a sophisticated optical and image detection system as well as an image analysis process. The graphene-material-based aqueous solution system and the graphene-material-based solid-phase system can be applied for different application purposes according to their features.

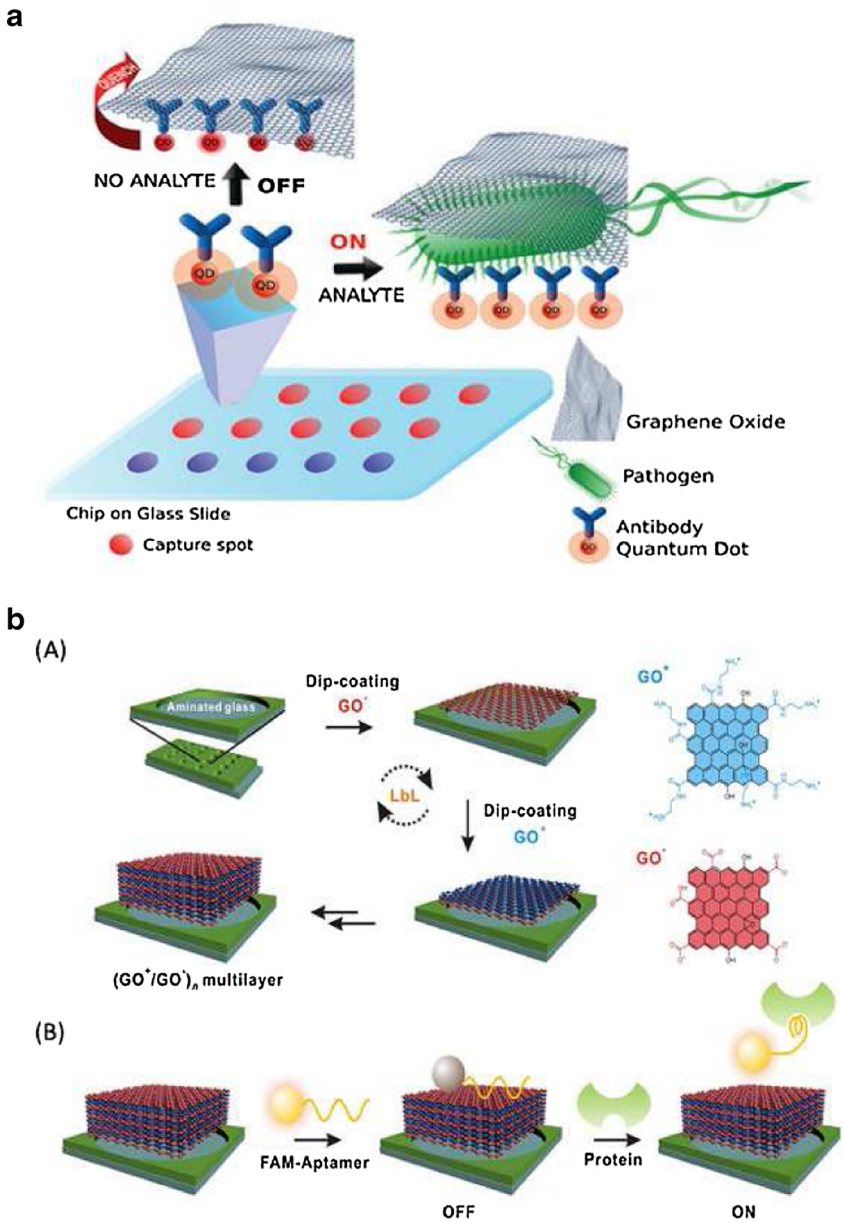

Fig. 8 **a** Antibody–QD microarrays for pathogen assay. In the presence of the pathogen, the quenching of the probes is minimal, as they barely interact with GO (on state); without the pathogen, the probes are quenched by electrostatic or π–π stacking interactions between the probes and GO (off state). **b** The layer-by-layer (*LbL*)-assembled GO multilayer array (*A*) and the aptamer-based protein sensing mechanism (*B*). (**a** From [131], copyright 2013 Wiley-VCH Verlag GmbH& Co. KGaA; **b** from [133], copyright 2013, rights managed by Nature Publishing Group)

Graphene–plasmonic hybrid material for optical sensors

Besides being used as a sensing element for optical sensors, graphene material can be used as a substrate to improve the performance of optical sensors when combined with plasmonic materials [137–139]. Graphene material combined with conventional plasmonic material such as noble metals can significantly improve the absorption (and interaction) with visible and IR light, which is only 2.3 % for graphene material solely. Hence, graphene–plasmonic hybrid devices show not only great promise for optical sensing in different transduction versions such as surface plasmon resonance and surface-enhanced Raman spectroscopy, but also possibilities for improving performance in fluorescence and FRET modes [140–144]. Moreover, because graphene material has the advantages of a large surface area and a rich conjugate structure for interaction with biomolecules, a surface plasmon resonance sensing strategy based on a graphene material substrate with noble metal materials has drawn a lot of attention in recent years; more information can be found in [139].

Research at the University of Manchester demonstrated much higher fields acting on the molecules studied when using graphene–plasmonic hybrid devices. Schedin et al. [145] studied surface-enhanced Raman spectra of graphene obtained by depositing arrays of AuNPs of well-defined dimensions on a graphene/SiO_2 (300 nm)/Si system and detected significant enhancement at 633 nm. They achieved very high sensitivity (an areal mass sensitivity at a level of

femtograms per square millimeter and detection of individual biomolecules, respectively) using a graphene substrate functionalized with a nanoarray of AuNPs. The results suggested that graphene–plasmonic hybrid devices could provide unrivalled sensitivity on the single-molecule level by careful design. The results demonstrated graphene–plasmonic hybrid material holds great potential for the development of simple and ultrasensitive label-free biosensing technology [146, 147].

Conclusions and future perspectives

In conclusion, graphene material has been widely used in optical sensors for numerous analytes and has achieved great success. The most important sensing approach is based on the energy transfer mechanism; graphene material can be used either as an energy acceptor or as an energy donor for FRET sensors. Owing to its extraordinary properties such as large surface area, strong quenching ability at different wavelengths, and great biocompatibility (for some derivatives such as GO and GQDs), graphene material has shown many advantages in optical sensing: high sensitivity can be achieved owing to the high quenching efficiency of graphene material; excellent biocompatibility and being rich in functional groups make it possible to conveniently connect graphene material to biomolecules; the large surface area and strong quenching ability make the material capable of labeling multifluorophore probes for multicomponent assays; the donor–bridge–acceptor system makes possible easy sensor design. Researchers have conducted much theoretical and experimental research and have made significant progress in the optical sensor area. However, there are still some challenges:

1. Researchers tend to assign the FRET mechanism to the sensor, but the energy transfer process may follow another mechanism. Theoretical study of the energy transfer mechanism is important and should not be neglected.
2. The reproducibly of graphene material fabrication needs to be improved since different batches may produce a single layer or several layers of graphene and graphene with different surface properties, which is not favorable for research and application.
3. High salt concentration may cause aggregation and precipitation of graphene material, which may restrict its application in some enzyme reaction systems.

Although many optical sensors have been developed based on graphene material, there are still many applications to explore for graphene-material-based optical sensors. The optical sensors developed mainly use a labeling strategy and are focused on in vitro analysis. Developing more label-free optical sensors will be very useful. Besides, graphene-material-based optical sensors hold great potential for in vivo sensing and imaging because of the great biocompatibility and optical properties of graphene material. In addition, graphene–plasmonic hybrid material is worth exploring for the development of simple and ultrasensitive label-free optical sensors.

Acknowledgment We acknowledge support from National Natural Science Foundation of China (21025521, 21705034, and 21190041).

References

1. Allen MJ, Tung VC, Kaner RB (2009) Chem Rev 110:132–145
2. Novoselov KS, Geim AK, Morozov SV, Jiang D, Zhang Y, Dubonos SV, Grigorieva IV, Firsov AA (2004) Science 306:666–669
3. Novoselov KS, Geim AK, Morozov SV, Jiang D, Katsnelson MI, Grigorieva IV, Dubonos SV, Firsov AA (2005) Nature 438:197–200
4. Feng LY, Wu L, Qu XG (2013) Adv Mater 25:168–186
5. Bitounis D, Ali-Boucetta H, Hong BH, Min DH, Kostarelos K (2013) Adv Mater 25:2258–2268
6. Xu B, Ma K, Zhang J, Yang B, Tian W (2013) Nanoscale 5:7776–7779
7. Qian J, Wang D, Cai FH, Xi W, Peng L, Zhu ZF, He H, Hu ML, He S (2012) Angew Chem Int Ed 51:10570–10575
8. Hong H, Yang K, Zhang Y, Engle JW, Feng LZ, Yang YN, Nayak TR, Goel S, Bean J, Theuer CP, Barnhart TE, Liu Z, Cai WB (2012) ACS Nano 6:2361–2370
9. Yang K, Feng LZ, Shi XZ, Liu Z (2013) Chem Soc Rev 42:530–547
10. Xiang QJ, Yu JG, Jaroniec M (2012) Chem Soc Rev 41:782–796
11. Mao HY, Laurent S, Chen W, Akhavan O, Imani M, Ashkarran AA, Mahmoudi M (2013) Chem Rev 113:3407–3424
12. Pumera M (2011) Mater Today 14:308–315
13. Morales-Narváez E, Merkoçi A (2012) Adv Mater 24:3298–3308
14. Li Z, He MY, Xu DD, Liu ZH (2014) J Photochem Photobiol C 18:1–17
15. Zhang Y, Guo YM, Xianyu YL, Chen WW, Zhao YY, Jiang XY (2013) Adv Mater 25:3802–3819
16. Sapsford KE, Berti L, Medintz IL (2006) Angew Chem Int Ed 45:4562–4588
17. Chen GW, Song FL, Xiong XQ, Peng XJ (2013) Ind Eng Chem Res 52:11228–11245
18. Wang Y, Li ZH, Hu DH, Lin CT, Li JH, Lin YH (2010) J Am Chem Soc 132:9274–9276
19. He SJ, Song B, Li D, Zhu CF, Qi WP, Wen YQ, Wang LH, Song SP, Fang HP, Fan CH (2010) Adv Funct Mater 20:453–459
20. Ocsoy I, Gulbakan B, Chen T, Zhu GZ, Chen Z, Sari MM, Peng L, Xiong XL, Fang XH, Tan WH (2013) Adv Mater 25:2319–2325
21. Huang JH, Zheng QB, Kim JK, Li ZG (2013) Biosens Bioelectron 43:379–383
22. Li F, Pei H, Wang LH, Lu JX, Gao JM, Jiang BW, Zhao XC, Fan CH (2013) Adv Funct Mater 23:4140–4148
23. Selvin PR (2000) Nat Struct Biol 7:730–734
24. Clapp AR, Medintz IL, Mauro JM, Fisher BR, Bawendi MG, Mattoussi H (2004) J Am Chem Soc 126:301–310
25. Swathi RS, Sebastian KL (2009) J Chem Phys 130:086101
26. Swathi RS, Sebastian KL (2008) J Chem Phys 129:054703
27. Li M, Zhou XJ, Guo SW, Wu NQ (2013) Biosens Bioelectron 43:69–74
28. Lu CH, Yang HH, Zhu CL, Chen X, Chen GN (2009) Angew Chem Int Ed 48:4785–4787
29. Miyahata T, Kitamura Y, Futamura A, Matsuura H, Hatakeyama K, Koinuma M, Matsumoto Y, Ihara T (2013) Chem Commun 49:10139–10141

30. Huang PJ, Liu JW (2012) Anal Chem 84:4192–4198
31. Tao Y, Lin YH, Huang ZZ, Ren JS, Qu XG (2012) Analyst 137: 2588–2592
32. Dong HF, Gao WC, Yan F, Ji HX, Ju HX (2010) Anal Chem 82: 5511–5517
33. Lu CH, Li J, Qi XJ, Song XR, Yang HH, Chen X, Chen GN (2011) J Mater Chem 21:10915–10919
34. Xiang X, Luo M, Shi LY, Ji XH, He ZK (2012) Anal Chim Acta 751:155–160
35. Dong HF, Zhang J, Ju HX, Lu HT, Wang SY, Jin S, Hao KH, Du HW, Zhang XJ (2012) Anal Chem 84:4587–4593
36. Cui L, Lin XY, Lin NH, Song YL, Zhu Z, Chen X, Yang CYJ (2012) Chem Commun 48:194–196
37. Jang H, Ryoo SR, Kim YK, Yoon S, Kim H, Han SW, Choi BS, Kim DE, Min DH (2013) Angew Chem Int Ed 52:2340–2344
38. Huang J, Yang XH, He XX, Wang KM, He Y, Quan K (2013) Chem Commun 49:9827–9829
39. Huang PJJ, Liu J (2012) Small 8:977–983
40. Mohanty N, Berry V (2008) Nano Lett 8:4469–4476
41. Chang HX, Tang LH, Wang Y, Jiang JH, Li JH (2010) Anal Chem 82:2341–2346
42. Liu XQ, Wang F, Aizen R, Yehezkeli O, Willner I (2013) J Am Chem Soc 135:11832–11839
43. Wu SJ, Duan N, Ma XY, Xia Y, Wang HX, Wang ZP, Zhang Q (2012) Anal Chem 84:6263–6270
44. Liu CH, Wang Z, Jia HX, Li ZP (2011) Chem Commun 47:4661–4663
45. Zhen SJ, Zhuang HL, Wang J, Huang CZ (2013) Anal Methods 5: 6904–6907
46. Yi M, Yang S, Peng ZY, Liu CH, Li JS, Zhong WW, Yang RH, Tan WH (2014) Anal Chem 86:3548–3554
47. Li X, Ma K, Zhu SJ, Yao SY, Liu ZY, Xu B, Yang B, Tian WJ (2014) Anal Chem 86:298–303
48. Zhang P, Wang Y, Leng F, Xiong ZH, Huang CZ (2013) Talanta 112:117–122
49. Bai YF, Feng F, Zhao L, Chen ZZ, Wang HY, Duan YL (2014) Analyst 139:1843–1846
50. Sun WL, Shi S, Yao TM (2011) Anal Methods 3:2472–2474
51. Liu JJ, Song XR, Wang YW, Chen GN, Yang HH (2012) Nanoscale 4:3655–3659
52. Liu XQ, Aizen R, Aizen R, Freeman R, Yehezkeli O, Willner I (2012) ACS Nano 6:3553–3563
53. Wang L, Zhu JB, Han L, Jin LH, Zhu CZ, Wang E, Dong SJ (2012) ACS Nano 6:6659–6666
54. Wang Y, Li Z, Weber TJ, Hu D, Lin CT, Li J, Lin Y (2013) Anal Chem 85:6775–6782
55. Zheng J, Nie YH, Hu YP, Li JS, Li YH, Jiang Y, Yang RH (2013) Chem Commun 49:6915–6917
56. MacLean JL, Morishita K, Liu JW (2013) Biosens Bioelectron 48: 82–86
57. Wang YX, Li JS, Wang H, Jin JY, Liu JH, Wang K, Tan WH, Yang RH (2010) Anal Chem 82:6607–6612
58. Xie WY, Huang WT, Li NB, Luo HQ (2012) Chem Commun 48: 82–84
59. Wen YQ, Xing FF, He SJ, Song SP, Wang LH, Long YT, Li D, Fan CH (2010) Chem Commun 46:2596–2598
60. Gao Y, Li Y, Zou X, Huang H, Su XG (2012) Anal Chim Acta 73: 68–74
61. Liu H, Wang Y, Shen A, Zhou X, Hu J (2012) Talanta 93:330–335
62. Zhang M, Ye BC (2012) Chem Commun 48:3647–3649
63. Santoro SW, Joyce GF, Sakthivel K, Gramatikova S, Barbas CF (2000) J Am Chem Soc 122:2433–2439
64. Brown AK, Li J, Pavot CM, Lu Y (2003) Biochemistry 42:7152–7161
65. Xiang Y, Tong AJ, Lu Y (2009) J Am Chem Soc 131:15352–15357
66. Hao YL, Guo QQ, Wu HY, Guo LQ, Zhong LS, Wang J, Lin TR, Fu FF, Chen GN (2014) Biosens Bioelectron 52:261–264
67. Zhang XB, Kong RM, Lu Y (2011) Annu Rev Anal Chem 4:105–128
68. Liu M, Zhao HM, Chen S, Yu HT, Zhang XB, Quan X (2011) Biosens Bioelectron 26:4111–4116
69. Zhao XH, Kong RM, Zhang XB, Meng HM, Liu WN, Tan WH, Shen GL, Yu RQ (2011) Anal Chem 83:5062–5066
70. Liu M, Zhao HM, Chen S, Yu HT, Zhang XB, Quan X (2011) Chem Commun 47:7749–7751
71. Yin BC, Ye BC, Tan WH, Wang H, Xie CC (2009) J Am Chem Soc 131:14624–14625
72. Liu JW, Lu Y (2007) J Am Chem Soc 129:9838–9839
73. Zhu WP, Zhao ZW, Li Z, Li H, Jiang JH, Shen GL, Yu RQ (2013) New J Chem 37:927–932
74. Peng L, Zhu Z, Chen Y, Han D, Tan WH (2012) Biosens Bioelectron 35:475–478
75. Liu YF, Luo M, Xiang X, Chen CH, Ji XH, Chen L, He ZK (2014) Chem Commun 50:2679–2681
76. Zhao XH, Ma QY, Wu XX, Zhu X (2012) Anal Chim Acta 727:67–70
77. Wang HB, Ou LJ, Huang KJ, Wen XG, Wang LL, Liu YM (2013) Can J Chem 91:1266–1271
78. Li W, Wu P, Zhang H, Cai C (2012) Anal Chem 84:7583–7590
79. Zhang H, Li Y, Su XG (2013) Anal Biochem 442:172–177
80. Lee J, Kim YK, Min DH (2011) Anal Chem 83:8906–8912
81. Tang LH, Chang HX, Liu Y, Li JH (2012) Adv Funct Mater 22: 3083–3088
82. Li Z, Zhu WP, Zhang JW, Jiang JH, Shen GL, Yu RQ (2013) Analyst 138:3616–3620
83. Zhu DB, Xing XB, Ma WG, Lu SQ, Su BH (2014) Sensors Actuators B 193:178–184
84. Qiu L, Zhou H, Zhu WP, Qiu LP, Jiang JH, Shen GL, Yu RQ (2013) New J Chem 37:3998–4003
85. Liu P, Yang XH, Sun S, Wang Q, Wang KM, Huang J, Liu JB, He LL (2013) Anal Chem 85:7689–7695
86. Yang L, Liu CH, Ren W, Li ZP (2012) Appl Mater Interfaces 4: 6450–6453
87. Huang JH, Gao X, Jia JJ, Kim JK, Li ZG (2014) Anal Chem 86: 3209–3215
88. Aragay G, Pino F, Merkoçi A (2012) Chem Rev 112:5317–5338
89. Tang D, Hou L, Niessner R, Xu M, Gao Z, Knopp D (2013) Biosens Bioelectron 46:37–43
90. Penn MA, Drake DM, Driskell JD (2013) Anal Chem 85:8609–8617
91. Wang JS, Qu XG (2013) Nanoscale 5:3589–3600
92. Liu M, Zhao HM, Quan X, Chen S, Fan XF (2010) Chem Commun 46:7909–7911
93. Chen L, Zhang XW, Zhou GH, Xiang X, Ji XH, Zheng ZH, He ZK, Wang HZ (2012) Anal Chem 84:3200–3207
94. Liu ZF, Jiang LH, Galli F, Nederlof I, Olsthoorn RCL, Lamers GEM, Oosterkamp TH, Abrahams JP (2010) Adv Funct Mater 20:2857–2865
95. Zhang CL, Yuan YX, Zhang SM, Wang YH, Liu ZH (2011) Angew Chem Int Ed 50:6851–6854
96. Alava T, Mann JA, Theodore C, Benitez JJ, Dichtel WR, Parpia JM, Craighead HG (2013) Anal Chem 85:2754–2759
97. Chen QS, Wei WL, Lin JM (2011) Biosens Bioelectron 26:4497–4502
98. Wang LH, Pu KY, Li J, Qi XY, Li H, Zhang H, Fan CH, Liu B (2011) Adv Mater 23:4386–4391
99. De M, Chou SS, Dravid VP (2011) J Am Chem Soc 133:17524–17527
100. Katoch J, Kim SN, Kuang Z, Farmer BL, Naik RR, Tatulian SA, Ishigami M (2012) Nano Lett 12:2342–2346
101. Ou L, Luo Y, Wei G (2011) J Phys Chem B 115:9813–9822
102. Mann JA, Alava T, Craighead HG, Dichtel WR (2013) Angew Chem Int Ed 52:3177–3180

103. Mann JA, Dichtel WR (2013) J Phys Chem Lett 4:2649–2657
104. Wang Z, Huang P, Bhirde A, Jin A, Ma Y, Niu G, Neamati N, Chen XY (2012) Chem Commun 48:9768–9770
105. Wang XH, Wang CY, Qu KG, Song YJ, Ren JS, Miyoshi D, Sugimoto N, Qu XG (2010) Adv Funct Mater 20:3967–3971
106. Feng BY, Guo LJ, Wang LH, Li F, Lu JX, Gao JM, Fan CH, Huang Q (2013) Anal Chem 85:7732–7737
107. Wang HB, Zhang Q, Chu X, Chen TT, Ge J, Yu RQ (2011) Angew Chem Int Ed 50:7065–7069
108. Rajesh C, Majumder C, Mizuseki H, Kawazoe Y (2009) J Chem Phys 130:124911
109. Zhang M, Yin BC, Wang XF, Ye BC (2011) Chem Commun 47:2399–2401
110. Li J, Lu CH, Yao QH, Zhang XL, Liu JJ, Yang HH, Chen GN (2011) Biosens Bioelectron 26:3894–3899
111. Feng D, Zhang YY, Feng TT, Shi W, Li XH, Ma HM (2011) Chem Commun 47:10680–10682
112. Zhu SJ, Tang SJ, Zhang JH, Yang B (2012) Chem Commun 48:4527–4539
113. Jung JW, Cheon DS, Liu F, Lee KB, Seo TS (2010) Angew Chem Int Ed 49:5708–5711
114. Liu F, Choi JY, Seo TS (2010) Biosens Bioelectron 25:2361–2365
115. Huang XY, Lan T, Zhang BC, Ren JC (2012) Analyst 137(16):3659–3666
116. Fu XL, Lou TT, Chen ZP, Lin M, Feng WW, Chen LX (2012) ACS Appl Mater Interfaces 4(2):1080–1086
117. Shi Y, Wu JZ, Sun YJ, Zhang Y, Wen ZW, Dai HC, Wang HD, Li Z (2012) Biosens Bioelectron 38:31–36
118. Kuila T, Bose S, Khanra P, Mishrab AK, Kim NH, Lee JH (2011) Biosens Bioelectron 26:4637–4648
119. Zhang YB, Petibone D, Xu Y, Mahmood M, Karmakar A, Casciano D, Ali S, Biris AS (2014) Drug Metab Rev 46:232–246
120. Kundu A, Layek RK, Kuila A, Nandi AK (2012) ACS Appl Mater Interfaces 4:5576–5582
121. Liu F, Ha HD, Han DJ, Seo TS (2013) Small 9:3410–3414
122. Luo Z, Vora PM, Mele EJ, Johnson ATC, Kikkawa JM (2009) Appl Phys Lett 94:111909
123. Ponomarenko LA, Schedin F, Katsnelson MI, Yang R, Hill EW, Novoselov KS, Geim AK (2008) Science 320:356–358
124. Dong YQ, Li GL, Zhou NN, Wang RX, Chi YW, Chen GN (2012) Anal Chem 84:8378–8382
125. Lin LP, Rong MC, Luo F, Chen DM, Wang YR, Chen X (2014) Trends Anal Chem 54:83–102
126. Zhao HM, Chang YY, Liu M, Gao S, Yu HT, Quan X (2013) Chem Commun 49:234–236
127. Shen JH, Zhu YH, Yang XL, Li CZ (2012) Chem Commun 48:3686–3699
128. Ran X, Sun H, Pu F, Ren J, Qu X (2013) Chem Commun 49:1079–1081
129. Sun HJ, Wu L, Wei WL, Qu XG (2013) Mater Today 16:434–442
130. Morales-Narváez E, Pérez-López B, Pires LB, Merkoçi A (2012) Carbon 50:2987–2993
131. Morales-Narváez E, Hassan AR, Merkoç IA (2013) Angew Chem Int Ed 52:13779–13783
132. Myung S, Solanki A, Kim C, Park J, Kim KS, Lee KB (2011) Adv Mater 23:2221–2225
133. Jung YK, Lee T, Shin E, Kim BS (2013) Sci Rep 3:3367
134. Furukawa K, Ueno Y, Tamechika E, Hibino H (2013) J Mater Chem B 1:1119–1124
135. Lee DW, Hong TK, Kang DW, Lee J, Heo M, Kim JY, Kim BS, Shin HS (2011) J Mater Chem 21:3438–3442
136. Hwang H, Joo P, Kang MS, Ahn G, Han JT, Kim BS, Cho JH (2012) ACS Nano 6:2432–2440
137. Grigorenko AN, Polini M, Novoselov KS (2012) Nat Photonics 6:749–758
138. Luo XG, Qiu T, Lu WB, Ni ZH (2013) Mater Sci Eng R 74:351–376
139. Szunerits S, Maalouli N, Wijaya E, Vilcot JP, Boukherroub R (2013) Anal Bioanal Chem 405:1435–1443
140. Fan Z, Kanchanapally R, Ray PC (2013) J Phys Chem Lett 4:3813–3818
141. Murphy S, Huang L, Kamat PV (2013) J Phys Chem C 117:4740–4747
142. Thrall ES, Crowther AC, Yu Z, Brus LE (2012) Nano Lett 12:1571–1577
143. Xu W, Ling X, Xiao J, Dresselhaus MS, Kong J, Xu H, Liu Z, Zhang J (2012) Proc Natl Acad Sci U S A 109:9281–9286
144. Lu G, Li H, Liusman C, Yin ZY, Wu SX, Zhang H (2011) Chem Sci 2:1817–1821
145. Schedin F, Lidorikis E, Lombardo A, Kravets VG, Geim AK, Grigorenko AN, Novoselov KS, Ferrari AC (2010) ACS Nano 4:5617–5626
146. Kravets VG, Schedin F, Jalil R, Britnell L, Novoselov KS, Grigorenko AN (2012) J Phys Chem C116:3882–3887
147. Kravets VG, Schedin F, Jalil R, Britnell L, Gorbachev RV, Ansell D, Thackray B, Novoselov KS, Geim AK, Kabashin AV, Grigorenko AN (2013) Nat Mater 12:304–309